



Efficient neural network- and tree-based machine learning models for predicting shear capacity of RC slender walls

Sy-Minh Nguyen¹ · Ngoc-Long Tran² · Trong-Ha Nguyen² · Van-Binh Tran¹ · Duy-Duan Nguyen²

Received: 4 December 2023 / Accepted: 18 January 2024 / Published online: 4 March 2024
© The Author(s), under exclusive licence to Springer Nature Switzerland AG 2024

Abstract

Slender reinforced concrete (RC) walls are popularly employed to improve the lateral loading capacity of high-rise buildings. Shear strength is an important target in designing RC walls subjected to horizontal loads such as earthquakes. This study aims to develop machine learning (ML) models for estimating the shear capacity of RC slender walls. A total of 154 test results, which were published in the literature, are gathered for training ML models. Two neural network-based models, i.e., Artificial neural network- Levenberg Marquardt (ANN-LM) and Artificial neural network-Bayesian regularization (ANN-BR), and two tree-based ML models including Random Forest (RF) and Gradient boosting regression tree (GBRT), are developed to predict the shear strength of RC walls. The predicted results obtained from ML models are then compared with those from empirical formulas in design codes. It shows that ML models are superior in predicting the shear capacity of RC slender walls compared to other code-based models, especially, RF and GBRT highly efficient models. Moreover, a practical graphical user interface tool is proposed to simplify the practical design of RC slender walls.

Keywords RC slender wall · Shear strength · Artificial neural network · Random Forest · Gradient boosting regression tree · Graphical user interface

Introduction

Slender reinforced concrete (RC) walls are commonly utilized in high-rise buildings for improving horizontal loading capacity. So far, numerous design codes and previous studies have proposed formulas to estimate the shear strength of RC walls including slender and squat types, in which typical code-based formulas are from ACI 318 (2014), ASCE/

SEI-43 (2005), and EC8 (2004). Additional, empirical-based formulas for calculating shear strength of squat RC walls can be found in well-known studies (Adorno-Bonilla, 2016; Gulec & Whittaker, 2011; Gulec et al., 2008; Kassem, 2015; Sánchez-Alejandre & Alcocer, 2010; Wood, 1990). However, those proposed formulas are mostly applied for squat RC walls.

So far, many studies have been performed to evaluate the shear strength of RC squat walls. Gulec and Whittaker (2011) proposed empirical formulas to calculate the shear capacity of RC walls with rectangular and flanged sections based on the results of 227 experimental data sets. Wood (1990) evaluated the nominal shear strength calculation formula in ACI 318–83 design standard based on 143 tested data sets of short RC walls subjected to lateral loads. Sánchez-Alejandre and Alcocer (2010) proposed a design model for calculating the shear strength of short RC walls subjected to earthquake loads. In the study of Kassem (2015), an analytical expression was derived to calculate the shear strength considering the influence of the diagonal concrete section and wall web reinforcement. The model parameters were calibrated using 664 experimental data sets of rectangular and flanged RC walls. Besides, some typical design standards have provided formulas to calculate the

✉ Duy-Duan Nguyen
duyduankxd@vinhuni.edu.vn

Sy-Minh Nguyen
minh.nguyensy@htu.edu.vn

Ngoc-Long Tran
longtn@vinhuni.edu.vn

Trong-Ha Nguyen
trongha@vinhuni.edu.vn

Van-Binh Tran
binh.tranvan@htu.edu.vn

¹ Department of Technology and Engineering, Ha Tinh University, Ha Tinh, Vietnam

² Department of Civil Engineering, Vinh University, Vinh 461010, Vietnam

shear capacity of rectangular-section walls including ACI 318 (2014), ASCE/SEI-43 (2005), and EC8 (2004). However, there are differences in the expressions of the standards, especially the application limits and accompanying assumptions.

Recently, numerous studies have applied machine learning (ML) for predicting performance of civil engineering structures (Chatterjee et al., 2017; Falcone et al., 2020; Kaveh & Khavaninzadeh, 2023; Kaveh et al., 2021, 2023; Thai, 2022). Some researchers used ML for estimating the shear strength and failure patterns of RC walls (Chen et al., 2018; Mangalathu et al., 2020; Moradi & Hariri-Ardebili, 2019). Chen et al. (2018) employed the ANN-PSO model to estimate the shear capacity of squat rectangular RC walls using 139 experimental samples. They emphasized that the ML model obtained the shear strength more accurately than other models. Nevertheless, it is challenged to apply this ML model for engineering designs due to lack of a practical tool. Moradi and Hariri-Ardebili (2019) developed a library of shear-wall database and then constructed a ANN model for estimating shear strength of generic RC walls. The results showed that the ANN model achieved good accuracy, however, practical tools such as graphic user interfaces (GUIs) or equations were not proposed. Nguyen et al. (2021) developed an effective ANN model for predicting shear strength of squat flanged RC walls. As a result, a mathematical equation and GUI were proposed. Keshtegar et al. (2021) combined the support vector regression (SVR) and response surface model (RSM) to predict the shear strength of RC walls with flanged sections. They emphasized that the hybrid ML model was more efficient compared to others. Tariq et al. (2022) developed gene expression programming (GEP) based on 646 data samples for predicting shear strength of RC squat walls. They showed that GEP was superior to empirical models. Chou et al. (2022) developed single and ensemble ML models to predict shear strength of RC walls with flanged sections using 492 samples. The proposed ensemble and optimized models were better than the single and empirical ones. Recently, Farzinpour et al. (2023) developed boosting learning algorithms for calculating strength capacity of flanged RC walls. Previous studies mostly focused on predicting the shear strength of RC squat/short walls. However, an accurate estimation of the shear strength for RC slender walls using ML models has not been investigated thoroughly. Additionally, practical tools for transferring ML models in engineering practices are required.

The purpose of this study is to construct efficient neural network- and tree-based ML models to accurately estimate the shear strength of RC slender walls. A total of 154 experiments, which were published in the literature, were gathered

for training ML models. Two powerful neural network-based models, i.e., Artificial neural network-Levenberg Marquardt (ANN-LM) and Artificial neural network-Bayesian regularization (ANN-BR), and two tree-based ML models including Random Forest (RF) and Gradient boosting regression tree (GBRT) were constructed to estimate the shear strength of RC slender walls. The results obtained from ML models were compared to those of two design codes formulas. Moreover, a graphical user interface was developed according to ML models to simplify the design practice of RC slender walls.

Code-based formulas for calculating shear strength of RC walls

This study investigated the formulas in two typical design standards including ACI 318 Chapter 11 (2014) and EC8 (2004). Details of these equations are presented as follows.

ACI 318 Chapter 11 (2014)

The shear strength of RC walls (V) is determined by the following expression.

$$V = V_c + V_s \leq 0.83 \sqrt{f'_c} t_w d \quad (1)$$

where

$$V_c = 0.27 \lambda \sqrt{f'_c} t_w d + \frac{Pd}{4l_w} \quad (2)$$

or

$$V_c = \left[0.05 \lambda \sqrt{f'_c} + \frac{l_w \left(0.1 \lambda \sqrt{f'_c} + 0.2 \frac{P}{l_w t_w} \right)}{\frac{M}{V} - \frac{l_w}{2}} \right] t_w d \quad (3)$$

$$V_s = \frac{A_w f_y d}{s} \quad (4)$$

$$d = 0.8 l_w \quad (5)$$

where V_c is strength provided by concrete; V_s is the strength provided by horizontal reinforcement; f'_c is the compressive strength of concrete; t_w is the web thickness; l_w is the length of web; P is axial load; A_w is area of horizontal reinforcement; f_y is the yield strength of reinforcement; s the spacing of horizontal reinforcement; λ is the coefficient considering the reduction of concrete.

EC8 (2004)

The shear strength of RC walls (V) according to EC8 is calculated by:

$$V = \left[\rho_h f_{yh} \left(\frac{M_n}{V_n l_w} - 0.3 \right) + \rho_v f_{yv} * \left(1.3 - \frac{M_n}{V_n l_w} \right) \right] t_w d_w \tag{6}$$

if $\frac{1.5P}{A_w f'_c} < 0.1$

$$V = \left[0.15 \sqrt{f'_c} + \rho_h f_{yh} \left(\frac{M_n}{V_n l_w} - 0.3 \right) + \rho_v f_{yv} * \left(1.3 - \frac{M_n}{V_n l_w} \right) \right] t_w d_w \tag{7}$$

if $\frac{1.5P}{A_w f'_c} > 0.1$

where $d_w = 0.8l_w$; $\frac{M_n}{V_n l_w}$ is the ratio of moment to shear force; ρ_h is the horizontal reinforcement ratio; ρ_v is the vertical reinforcement ratio; f_{yh} is the yield strength of horizontal reinforcement; f_{yv} is the yield strength of vertical reinforcement; A_w is the wall cross-section area.

Experimental database

A set of 154 experimental samples on rectangular RC slender walls was collected from published works. It should be noted that the data sets covered a very wide range of input parameters such as the slenderness, the axial compression ratio, and used material properties. Input design properties include the wall height (H_w), wall length (L_w), wall thickness (t_w), length of flange (L_f), thickness of flange

(t_f), vertical reinforcement ratio of flange (ρ_{vf}), horizontal reinforcement ratio of flange (ρ_{hf}), vertical reinforcement ratio of web (ρ_{vw}), horizontal reinforcement ratio of web (ρ_{hw}), yield strength of flange reinforcement (f_{yf}), yield strength of vertical reinforcement of web (f_{yvw}), yield strength of horizontal reinforcement of web (f_{ywh}), compressive strength of concrete (f'_c), and axial compression force (P). Meanwhile, the output target is the shear strength (V). Figure 1 illustrates RC slender walls. Table 1 statistically summarizes the collected database used in this study. Statistical properties are the minimum value (Min), maximum value (Max), average value (Mean), standard deviation (SD) and coefficient of variation (CoV). In this table, the first 15 parameters are input parameters, while the last parameter (V) is the output shear strength. The distributions of collected database are shown in Fig. 2.

Overview of ML models

In this study, two neural network- and two tree-based ML models were developed to predict the shear capacity of RC slender walls, in which ANN-LM, ANN-BR, RF, and GBRT were considered. Neural network- and tree-based ML models contain some typical beneficials such as easy interpretation and understanding, well-performing with both larger and less database, and successful application for classification and regression problems. Brief introduction of these models is presented as follows. A general flowchart of used ML models is shown in Fig. 3.

Fig. 1 Illustration of RC slender walls

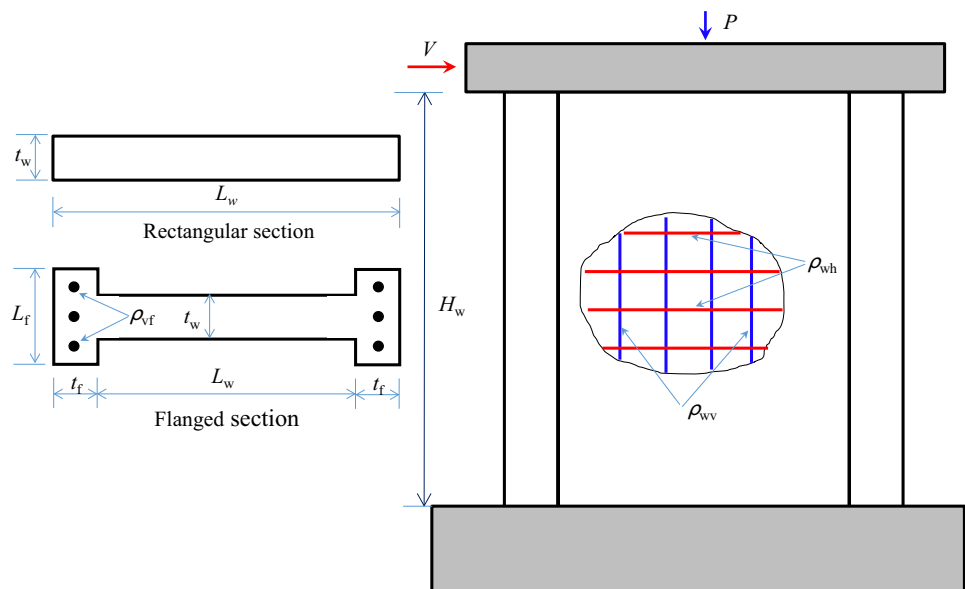


Table 1 Statistical summary of used database

Parameter	Units	Min	Mean	Max	SD	COV
H_w	mm	1067.00	3043.81	11,760.00	1580.22	0.52
L_w	mm	254.00	1221.69	2800.00	550.72	0.45
H_w/L_w	–	2.05	2.53	7.24	0.65	0.26
t_w	mm	50.00	115.30	300.00	50.71	0.44
L_f	mm	0.00	91.23	380.00	112.70	1.24
t_f	mm	0.00	129.59	914.00	182.43	1.41
ρ_{vf}	%	0.00	2.79	11.00	1.82	0.65
ρ_{hf}	%	0.00	0.82	3.58	0.81	0.99
ρ_{vw}	%	0.17	0.76	3.00	0.56	0.74
ρ_{hw}	%	0.00	0.63	2.45	0.45	0.72
f_{yf}	MPa	276.00	491.08	1412.00	152.33	0.31
f_{yvw}	MPa	276.00	487.88	1412.00	157.94	0.32
f_{ywh}	MPa	216.00	501.19	1412.00	164.13	0.33
f_c	MPa	12.30	42.19	130.80	18.19	0.43
P	kN	0.00	428.66	1764.00	433.93	1.01
V	kN	15.35	395.19	1062.00	296.26	0.75

ANN-LM

ANN-LM is the ML model, in which the Levenberg–Marquardt (LM) algorithm (Ranganathan, 2004) is combined with ANN to improve the prediction for engineering problems. The LM algorithm provides a stable convergence for training ANNs. Typical steps for implementing ANN-LM are as follows:

- (1) Data preparation: A large enough database is required to gather, in which cleaning and preprocessing steps for removing unnecessary characters and outliers.
- (2) Feature extraction: Based on the dataset input parameters are identified for building neural networks.
- (3) Model architecture: Design the architecture of ANN-LM with the input parameters, number of hidden layers, number of neurons in the hidden layer(s).
- (4) Training: Split the database into training and validation sets. Train ANN-LM model on the training set, using techniques like backpropagation and gradient descent to optimize the model's parameters. Adjust hyperparameters such as learning rate, batch size, and number of epochs to improve model performance.
- (5) Evaluation: Evaluate the performance of the trained model on the validation set using some typical statistical metrics such as mean squared error and goodness of fit.
- (6) Fine-tuning and iteration: Depending on the performance, the model can be fine-tuned by modifying hyperparameters or adjusting the architecture.
- (7) Testing: Since the model's performance is satisfied on the validation set, a test on unseen data is required to assess its generalization capability.

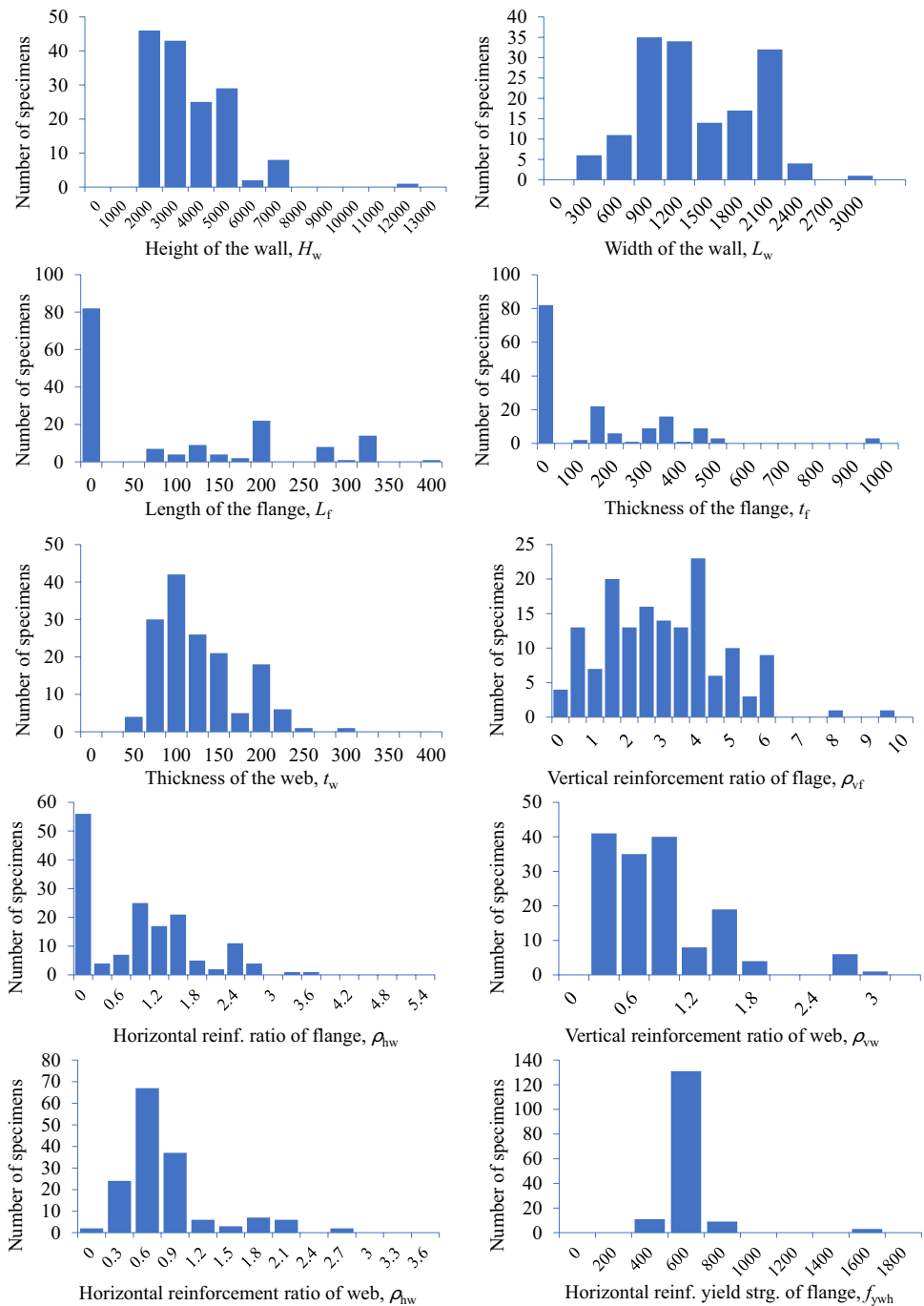
ANN-BR

The hybrid ANN-BR model combines the ANN and Bayesian regularization (BR) algorithm (Burden & Winkler, 2009). Bayes' theorem is employed to fine-tune the weights of the ANN model and optimize the loss function parameters in the training of ANN. As a result, the overfitting, an unexpected problem in training model, can be avoided. For performing the ANN-BR model, a similar procedure to the ANN-LM model can be adopted. The difference is that instead of using backpropagation, the Bayesian regression is applied to train the ANN model. This method considers uncertainty in the database, and then provide a better prediction (Nguyen & Nguyen, 2023).

RF

RF model is a powerful ML algorithm that's widely used for classification and regression tasks (Breiman, 2001). It's like a team of decision trees working together to make predictions. Firstly, it randomly selects a subset of the available features from the dataset. Then, it creates multiple decision trees using these subsets of features and different subsets of the training data. Each decision tree in RF independently predicts the outcome. To make a prediction, RF combines the predictions from all the decision trees and uses a voting mechanism (for classification) or averaging (for regression) to arrive at the final prediction. By aggregating the predictions of multiple trees, the RF model helps to reduce overfitting and improve the overall accuracy and robustness of the predictions. Typical flowing steps are required in performing the RF model.

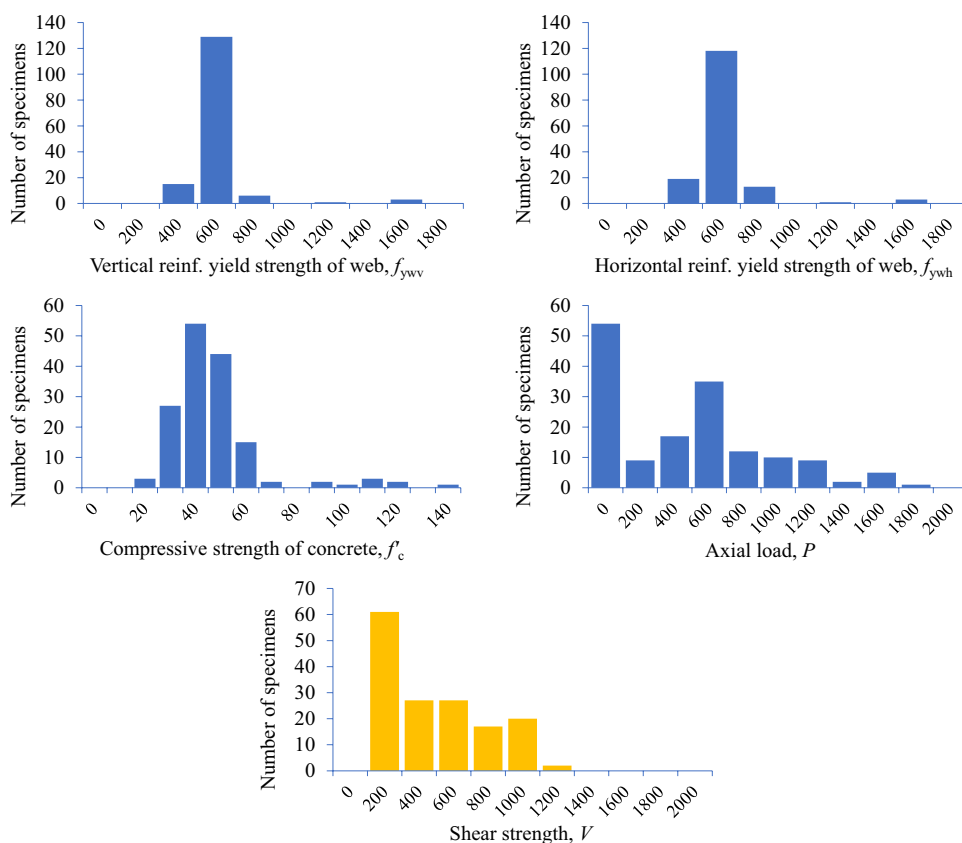
Fig. 2 Distribution of collected database



- (1) Gather and preprocess database: Collecting the dataset and ensuring it is properly formatted. This may involve cleaning missing values, handling categorical variables, and splitting the data into training and testing sets.
- (2) Choose the number of trees: Determining on the number of decision trees for RF model. This is a crucial hyperparameter that can affect the model’s performance.
- (3) Randomly select subsets of data: Randomly select subsets of the training data, with replacement. This process

- is known as bootstrapping. Each subset, also called a bootstrap sample, will be used to train an individual decision tree.
- (4) Build decision trees: For each bootstrap sample, construct a decision tree using a specific algorithm like CART (Classification and Regression Trees). Each tree is trained on a different subset of the data.
 - (5) Aggregate predictions: Once all the decision trees are built, predictions are made by each tree on the testing data. For classification tasks, the most common class

Fig. 2 (continued)



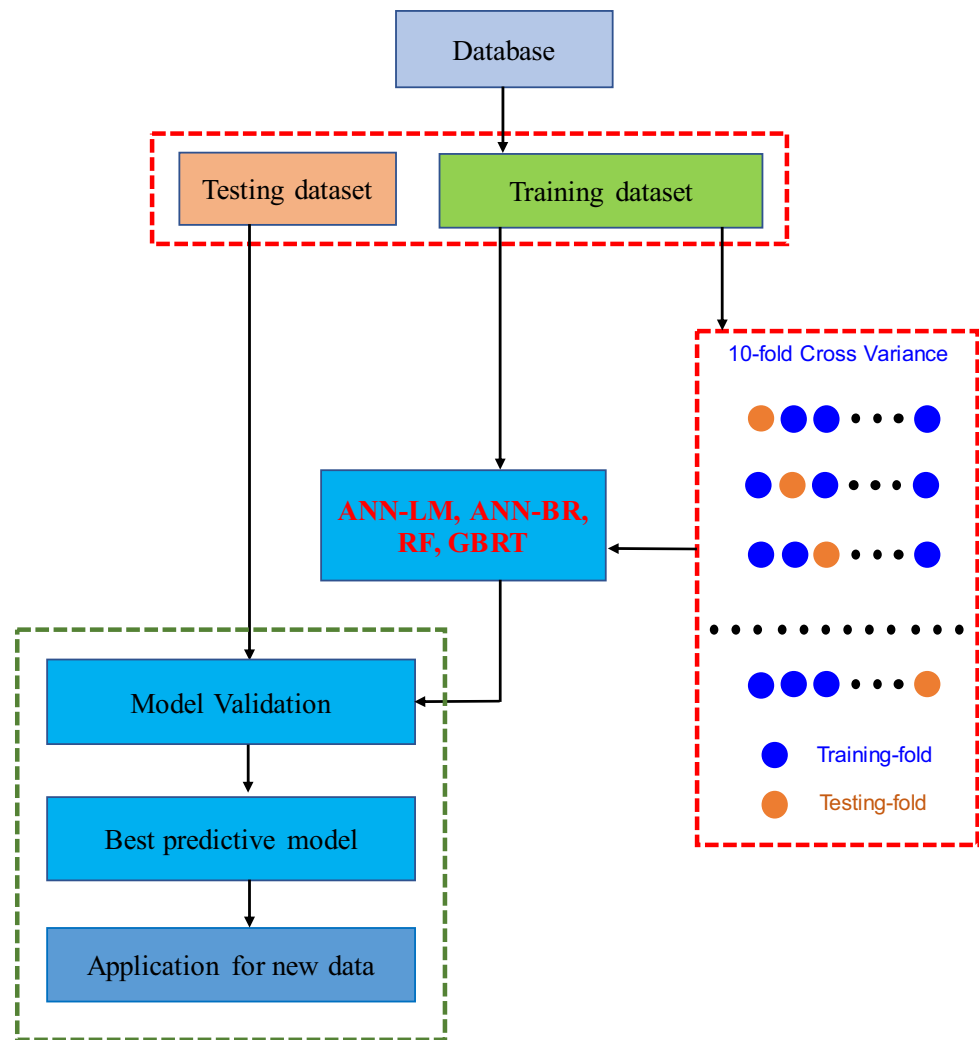
predicted by the trees is chosen as the final prediction. For regression tasks, the average of the predicted values is taken.

- (6) Evaluate the model: Assess the performance of the RF model using appropriate evaluation metrics such as accuracy, precision, recall, or mean squared error, depending on the problem type.
- (7) Fine-tune the model: Adjust the hyperparameters of the RF model, such as the number of trees or the maximum depth of each tree, to optimize its performance. This can be done using techniques like cross-validation or grid search.
- (8) Make predictions: Once the model is trained and fine-tuned, it can be used to make predictions on new data.

GBRT

GBRT model is the one of popular ML algorithms used for regression tasks. It combines the principles of gradient boosting and decision trees to solve regression problems (Chen & Guestrin, 2016). This model is also known as Gradient Boosting Machines or simply Gradient Boosting. Some key points in GBRT are:

- Ensemble method: GBRT is an ensemble method that combines multiple weak prediction models, typically decision trees, to create a strong predictive model. It builds the model in an iterative manner, where each new tree is trained to correct the mistakes made by the previous trees.
- Gradient boosting: GBRT uses gradient boosting, which is a technique that minimizes the loss function by iteratively adding new models to the ensemble. It focuses on reducing the errors made by the previous models by assigning higher weights to the misclassified instances.
- Decision trees: GBRT uses decision trees as the base models. Decision trees are constructed based on features and their corresponding target values. Each tree is built to predict the residuals (the differences between the actual and predicted values) of the previous trees.
- Sequential training: GBRT trains the trees in a sequential manner, where each tree is built to correct the errors made by the previous trees. The predictions of all the trees are combined to make the final prediction.
- Feature importance: GBRT provides a measure of feature importance, which indicates the relative importance of each feature in making predictions. This can be useful

Fig. 3 General flowchart of ML models

for feature selection and understanding the underlying patterns in the data.

- **Regularization:** GBRT models can be prone to overfitting, especially if the number of trees is too high. Regularization techniques, such as limiting the depth of the trees or adding a shrinkage parameter, can be applied to prevent overfitting and improve generalization.
- **Hyperparameter tuning:** GBRT models have several hyperparameters that can be tuned to optimize performance, such as the learning rate, number of trees, maximum depth of the trees, and the number of features considered at each split.

To conduct the GBRT model, the following typical steps are required.

- (1) **Gather and preprocess database:** Collect the datasets and ensure it is properly formatted. This may involve cleaning missing values, handling categorical vari-

ables, and splitting the data into training and testing sets.

- (2) **Choose the number of trees:** Decide on the number of regression trees in the GBRT model. This is an important hyperparameter that can affect the model's performance.
- (3) **Initialize the model:** Start by initializing the GBRT model with an initial prediction value. This can be a simple estimate, such as the mean or median of the target variable.
- (4) **Build the first tree:** Train the first regression tree using the training data. The tree is built to predict the residuals (the differences between the actual target values and the initial predictions) from the previous step.
- (5) **Update the model:** Update the model's predictions by adding the predictions from the first tree to the initial predictions. This creates a new set of predictions that are closer to the actual target values.
- (6) **Build subsequent trees:** Repeat steps 4 and 5 to build additional regression trees. Each tree is trained to pre-

dict the residuals from the previous step, and its predictions are added to the model's current predictions.

- (7) Define the learning rate: The learning rate is a hyperparameter that controls the contribution of each tree to the final predictions. It determines how much each tree's predictions are scaled before being added to the model. A lower learning rate makes the model more conservative, while a higher learning rate allows for more aggressive updates.
- (8) Evaluate the model: Assess the performance of the GBRT model using appropriate evaluation metrics such as mean squared error or R-squared. This can be done using the testing data.
- (9) Fine-tune the model: Adjust the hyperparameters of the GBRT model, such as the number of trees, the

learning rate, or the maximum depth of each tree, to optimize its performance. This can be done using techniques like cross-validation or grid search.

- (10) Make predictions: Once the model is trained and fine-tuned, it can be used to make predictions on new data.

Figures 4, 5, 6 and 7 show the performance of ANN-LM, ANN-BR, RF, and GBRT models, respectively. All ML models were trained with the training and testing ratio of 0.7 and 0.3, respectively. The RF and GBRT models were selected with training data ratios of 0.7 and 1000 trees. It can be observed that the predicted values were very close to the actual values (i.e., experimental values) for both ML models.

Fig. 4 Performance of ANN-LM

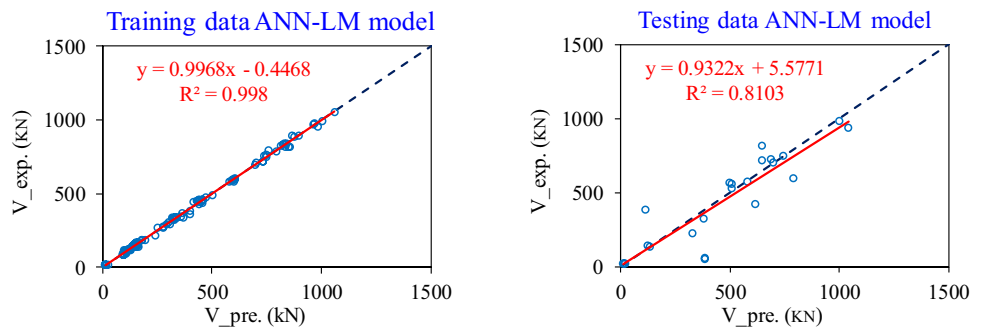


Fig. 5 Performance of ANN-BR

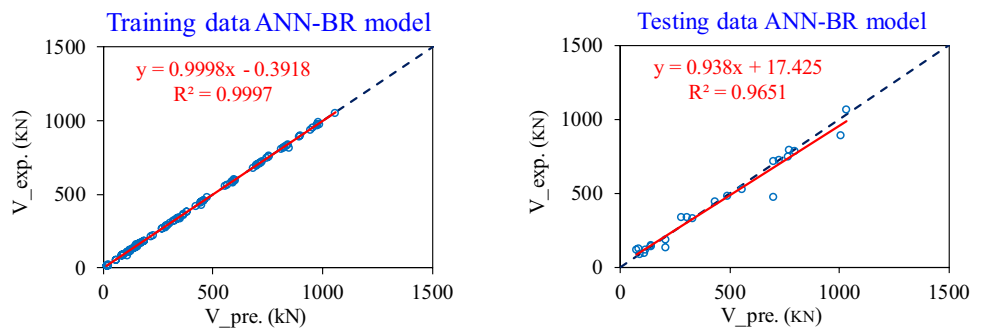


Fig. 6 Performance of RF model

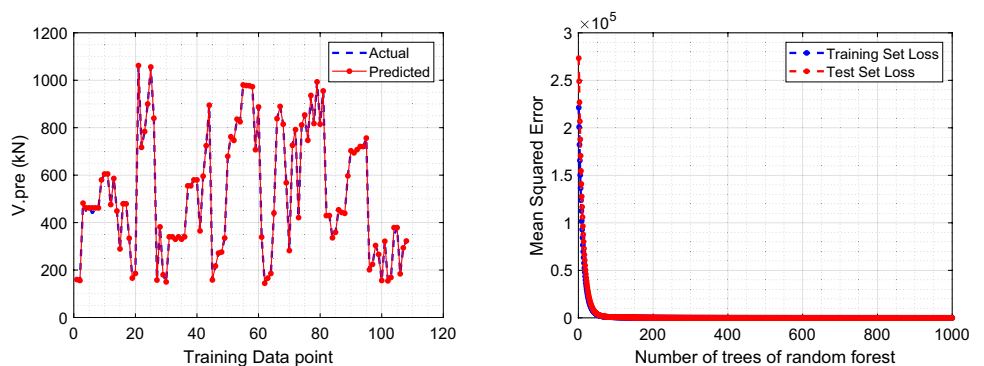
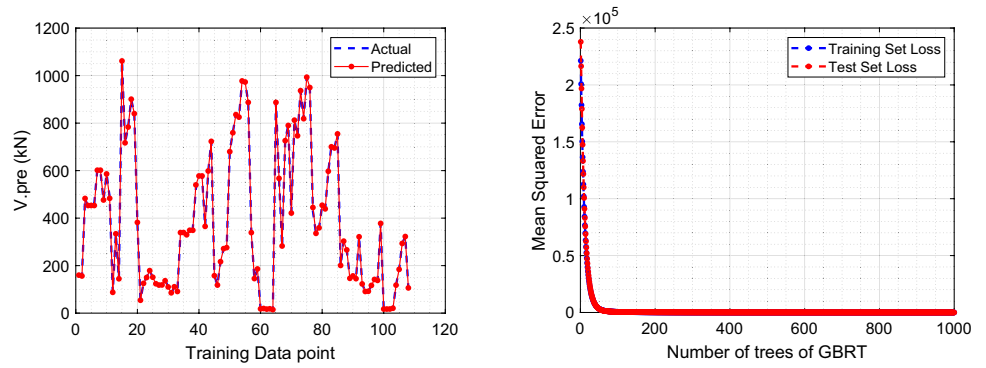


Fig. 7 Performance of GBRT model



Evaluation of predicted models for shear capacity of RC walls

The shear strength of RC slender walls is calculated according to two empirical formulas for the experimental database. Afterward, the shear strength obtained from design codes and two tree-based ML models are compared with that of the experiments. Figure 8 shows the comparison of

calculated shear strength of RC walls based on predictive models and experiments. It should be noted that the dashed line represents the perfect results, in which the predicted values are exactly equal to experiments. It was observed that shear strength results calculated by ACI-318 (2014) and EC8 (2004) show to be significantly scattered. This dispersion can be due to not taking account the boundary properties on

Fig. 8 Comparison of shear strength between predicted models and experiments

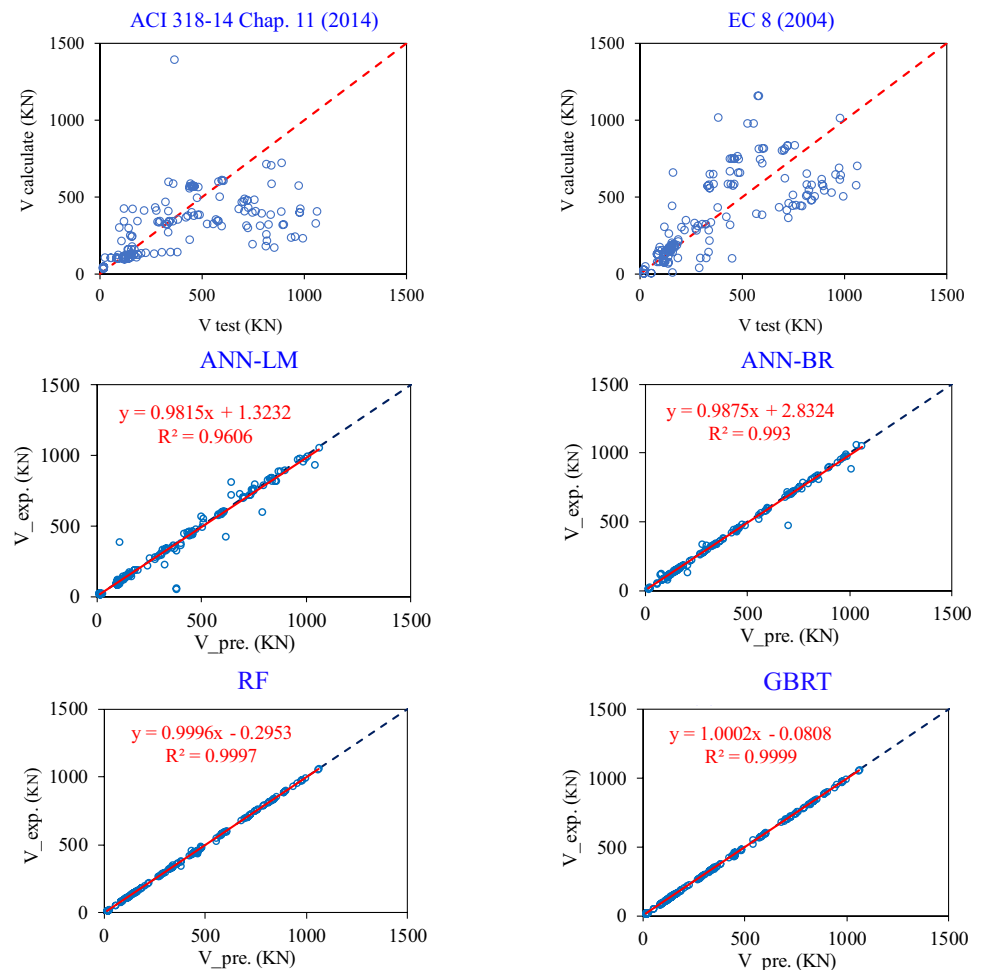
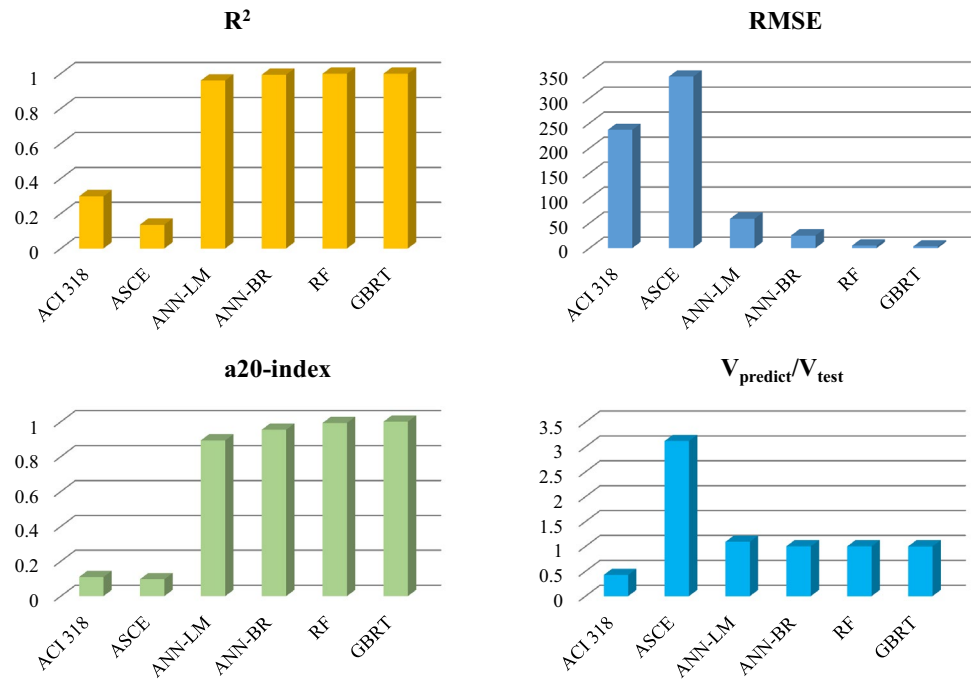


Fig. 9 Statistical values of different models**Table 2** Statistic indicators for evaluating predicted models

Model	R^2	a20-index	RMSE	$V_{predict}/V_{test}$				
				Min	Max	Mean	SD	CoV
ACI 318	0.298	0.110	436.5	0.047	2.258	0.427	0.352	0.825
EC 8	0.136	0.097	2743.2	0.906	23.156	3.119	2.658	0.852
ANN-LM	0.960	0.893	58.7	0.290	7.154	1.093	0.753	0.689
ANN-BR	0.993	0.954	25.3	0.609	1.484	1.003	0.092	0.092
RF	0.999	0.993	5.2	0.933	1.268	1.003	0.026	0.026
GBRT	0.999	1.000	3.3	0.880	1.116	1.000	0.019	0.019

the equations. Additionally, Fig. 8 shows that the ML models estimated shear strengths more accurately compared to the empirical models. Specifically, RF and GBRT achieved highly accurate predictions with R^2 values equal to 0.9997 and 0.9999, and very small RMSE of 5.2 kN and 3.3 kN, respectively.

Figure 9 and Table 2 show the calculated statistical indices including R^2 , RMSE, a20-index, and ratio between predicted and experimental strength ($V_{predict}/V_{test}$) for four predictive models. The results show that the ML models predicted the shear capacity of the RC wall more accurately compared with the empirical formulas. The RF and GBRT models emphasize the best performance with the highest R^2 (0.999), the lowest RMSE (~3.3 kN and 5.2 kN), and the average $V_{predict}/V_{test}$ ratio value was 1.0. The second-best predictive models are ANN-LM and ANN-BR. Meanwhile, the empirical models show a low accuracy in predicting the shear strength of RC slender walls.

Practical GUI tool

For employing the ML models in practical designs, a graphical user interface (GUI) is to be developed. A GUI tool based on RF and GBRT models is proposed to simplify the calculated process of the RC wall shear strength. Figure 10 illustrates the GUI tool in MATLAB, in which users can obtain the shear strength easily. Note that the prediction model is limited to the dataset provided in Table 1. The developed GUI tool can be downloaded freely at https://github.com/duyduan1304/GUI_RCslenderWalls.

Conclusions

Efficient neural network- and tree-based ML models were developed to estimate the shear strength of RC slender walls. A dataset of 154 experiments were collected and employed to train ML models. Four ML models were ANN-LM,

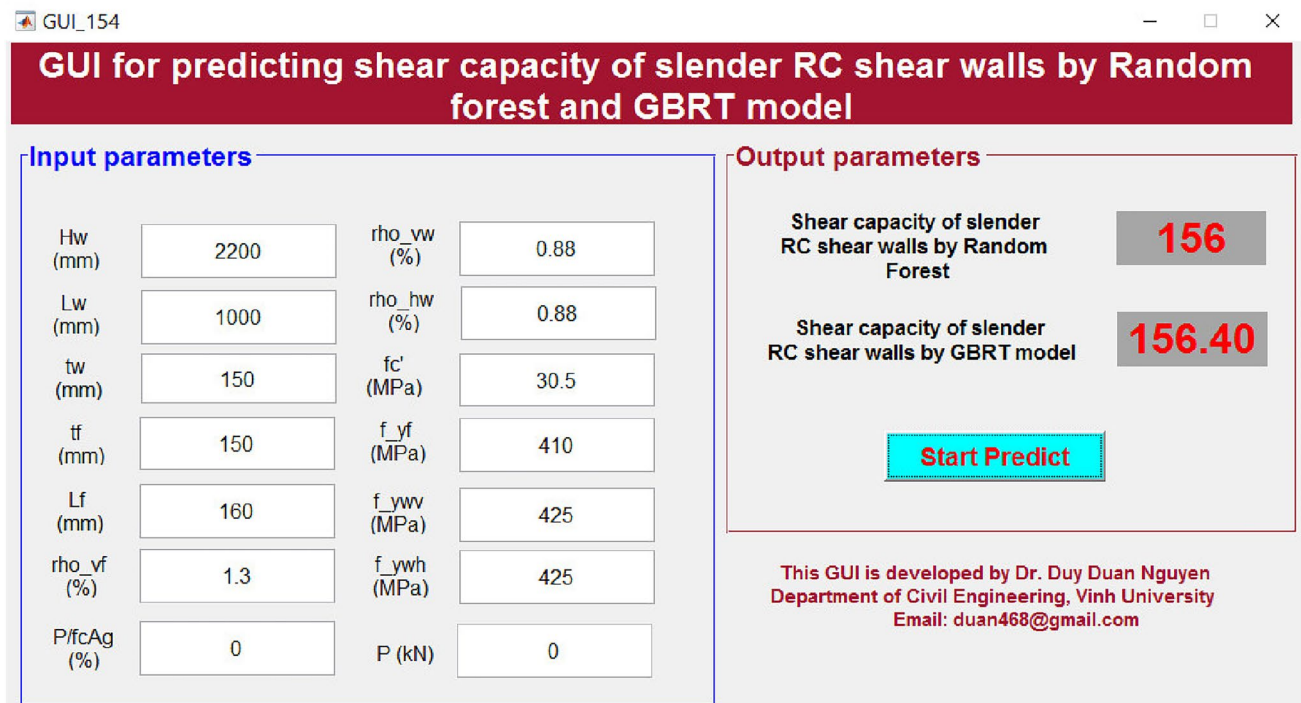


Fig. 10 GUI for estimating shear strength of RC slender walls

ANN-BR, RF, and GBRT. The predicted results obtained from ML models were compared with those of two empirical formulas in design codes (ACI 318 and Eurocode 8). The following conclusions are achieved.

- Neural network- and tree-based ML models accurately predicted the shear strength of RC slender walls, among that the RF and GBRT models were efficient to predict the shear strength with R^2 of 0.999 and small RMSE of 3 kN.
- Formulas of ACI-318 (2014) and EC8 (2004) obtained a large scattering results since it does not include the boundary element properties in calculated expressions.
- A graphical user interface was proposed based on efficient tree-based models to simplify the design practice of RC slender walls.

Appendix

Detailed information of the database

ID	H_w (mm)	L_w (mm)	t_w (mm)	H_w/L_w	t_f (mm)	L_f (mm)	ρ_{vf} (%)	ρ_{vw} (%)	ρ_{hw} (%)	f_c' (MPa)	f_{yf} (MPa)	f_{yvw} (MPa)	f_{ywh} (MPa)	P (kN)	V (kN)
1	11,760	1625	127	7.24	203	380	0.67	0.27	0.27	49	455	455	455	1500	160
2	2200	1000	150	2.20	150	160	1.3	0.88	0.88	30.5	410	425	425	0	156
3	1500	600	80	2.50	0	0	0.18	0.18	0.1	34.65	500	500	500	90	25
4	3450	1600	200	2.16	385	200	1.2	0.86	0.39	41.2	510	505	505	600	482
5	3450	1600	200	2.16	407	200	1.13	0.86	0.39	42.1	510	505	505	600	448
6	3450	1600	200	2.16	407	200	1.13	0.86	0.39	42.1	510	505	505	600	462
7	3450	1600	200	2.16	407	200	1.13	0.86	0.39	42.1	510	505	505	600	439
8	3450	1600	200	2.16	407	200	1.13	0.86	0.39	42.1	510	505	505	600	456
9	3450	1600	200	2.16	407	200	1.13	0.86	0.39	42.1	510	505	505	600	462

ID	H_w (mm)	L_w (mm)	t_w (mm)	H_w/L_w –	t_f (mm)	L_f (mm)	ρ_{vf} (%)	ρ_{vw} (%)	ρ_{hw} (%)	f_c' (MPa)	f_{yf} (MPa)	f_{yvw} (MPa)	f_{ywh} (MPa)	P (kN)	V (kN)
10	3650	1700	200	2.15	415	200	1.94	1.15	0.39	41.2	510	505	505	750	580
11	3650	1700	200	2.15	415	200	1.94	1.15	0.39	42.1	510	505	505	750	605
12	3650	1700	200	2.15	415	200	1.94	1.15	0.39	42.1	510	505	505	750	598
13	3550	1500	200	2.37	140	200	0.5	0.23	0.63	39.2	400	400	400	823.2	476
14	3550	1500	200	2.37	140	200	1.43	0.58	0.58	39.9	412	412	412	838	586
15	3550	1200	200	2.96	140	200	0	0.62	0	39.8	412	412	412	668.6	449
16	3550	1000	200	3.55	140	200	0	0.59	0	40.2	412	412	412	562.8	289
17	3250	1200	150	2.71	0	0	0.83	0.83	0.26	31.2	460	470	470	0	95
18	3250	1200	150	2.71	0	0	1.5	1.5	0.26	30.4	460	470	470	0	141
19	2700	1300	200	2.08	150	200	5.33	0.6	0.66	28.3	429	440	440	0	488
20	2700	1300	200	2.08	150	200	5.33	0.6	0.66	28.3	429	440	440	0	479
21	1140	548	84	2.08	60	200	2.36	0.48	0.66	47	437	437	437	0	87
22	1140	548	84	2.08	60	200	2.36	0.48	0.66	47	437	437	437	0	89
23	3900	1000	152	3.90	140	152	11	0.28	0.49	38.7	450	450	450	600	334
24	1600	700	100	2.29	140	100	0.45	0.72	0.44	27.4	469	445	445	287	144
25	1600	700	100	2.29	140	100	0.45	0.72	0.44	27.4	469	445	445	479	166
26	1600	700	100	2.29	140	100	0.45	0.72	0.44	27.4	469	445	445	671.6	186
27	3000	1300	80	2.31	200	200	2.13	0.53	0.53	87.6	776	1001	1001	1764	1062
28	3000	1300	80	2.31	200	200	2.13	0.265	0.265	55.5	713	753	753	1372	717
29	3000	1300	80	2.31	200	200	2.84	0.265	0.265	54.6	713	753	753	1568	784
30	3000	1300	80	2.31	200	200	2.84	0.53	0.53	60.3	713	753	753	1372	900
31	3000	1300	80	2.31	200	200	3.81	0.53	0.53	65.2	726	753	753	1568	1056
32	6400	2300	150	2.78	200	150	5	0.37	0.49	35.4	413	413.7	413.7	0	840
33	3800	1000	100	3.80	150	100	1.3	0.57	0.28	30	400	400	400	0	158
34	1800	880	240	2.05	0	0	0	1.19	1.28	40	500	500	500	0	382
35	2200	540	80	4.07	130	130	1.19	0.47	0.63	60	415	415	415	0	54
36	2200	540	80	4.07	130	130	1.19	0.47	0.63	60	415	415	415	0	55
37	1375	650	65	2.12	0	0	3.3	2.5	0.8	42.8	420	470	520	0	127
38	1375	650	65	2.12	0	0	3.3	2.5	0.8	50.6	420	470	520	182	150
39	1375	650	65	2.12	0	0	3.3	2.5	0.8	47.8	420	470	520	343	180
40	1375	650	65	2.12	0	0	3.3	2.5	0.8	48.3	420	470	520	0	120
41	1375	650	65	2.12	0	0	3.3	2.5	0.8	45	420	470	520	325	150
42	1375	650	65	2.12	0	0	3.3	2.5	0.4	30.1	420	470	520	0	123
43	1375	650	65	2.12	0	0	3.3	1.5	0.35	30.1	420	470	520	0	118
44	1375	650	65	2.12	0	0	3.3	1.5	0.35	35.2	420	470	520	0	116
45	1375	650	65	2.12	0	0	3.3	1.5	0.35	34.9	420	470	520	0	140
46	1375	650	65	2.12	0	0	3.3	1.5	0.35	53.6	420	470	520	0	111
47	1375	650	65	2.12	0	0	3.3	1.5	0.35	38.2	420	470	520	0	83
48	1375	650	65	2.12	0	0	3.3	1.5	0.35	49.2	420	470	520	0	112
49	1375	650	65	2.12	0	0	3.3	1.5	0.35	38.1	420	470	520	0	94
50	2500	1200	150	2.08	0	0	2.68	0.56	0.67	40	500	540	500	0	339
51	2500	1200	150	2.08	0	0	2.68	0.56	0.67	40	500	540	500	0	340
52	2500	1200	150	2.08	0	0	2.05	0.67	0.67	40	500	435	450	600	330
53	2500	1200	150	2.08	0	0	2.05	0.67	0.67	40	500	540	450	600	340
54	2500	1200	150	2.08	0	0	2.05	0.67	0.67	40	500	435	450	600	330
55	2500	1200	150	2.08	0	0	2.05	0.67	0.67	40	500	540	450	600	357
56	2500	1200	150	2.08	0	0	1.51	1.51	1.51	40	500	442	450	600	525
57	2500	1200	150	2.08	0	0	1.51	1.51	1.51	40	500	442	450	600	555
58	2500	1200	150	2.08	0	0	1.51	1.51	1.51	40	500	552	450	600	580
59	2500	1200	150	2.08	0	0	1.51	1.51	1.51	40	500	552	450	600	575

ID	H_w (mm)	L_w (mm)	t_w (mm)	H_w/L_w –	t_f (mm)	L_f (mm)	ρ_{vf} (%)	ρ_{vw} (%)	ρ_{hw} (%)	f_c' (MPa)	f_{yf} (MPa)	f_{yvw} (MPa)	f_{ywh} (MPa)	P (kN)	V (kN)
60	5750	2800	300	2.05	0	0	0.75	0.17	1.68	40.7	560	560	560	0	365
61	2200	1000	100	2.20	500	120	3.88	0.28	0.28	103.3	617	610	610	1012.34	596
62	2200	1000	100	2.20	500	120	3.88	0.75	0.28	96.8	617	578	610	948.64	724
63	2200	1000	100	2.20	500	120	3.88	0.28	0.75	110.7	617	610	578	1084.86	895
64	3810	1219	102	3.13	0	0	2.93	0.3	0.33	40.5	434	434	448	400.34	149
65	3810	1219	102	3.13	0	0	2.93	0.3	0.33	38.7	434	434	448	378.099	158
66	4572	1905	101.6	2.40	0	0	1.47	0.25	0.31	44.7	501.6	511	521.6	0	118
67	4572	1905	101.6	2.40	0	0	4	0.25	0.31	46.4	534.7	449	534.7	0	217
68	4572	1905	101.6	2.40	305	305	1.11	0.29	0.31	53	501.6	449	520.2	0	271
69	4572	1905	101.6	2.40	305	305	1.11	0.29	0.31	47.3	478.5	437	478.5	0	276
70	4572	1905	101.6	2.40	305	305	1.11	0.29	0.31	45	504.7	449	504.3	0	335
71	4572	1905	101.6	2.40	305	305	3.67	0.29	0.63	53.6	501.6	410	531.9	0	680
72	4572	1905	101.6	2.40	305	305	3.67	0.29	0.63	45.3	501.6	443	501.6	0	762
73	4572	1905	101.6	2.40	305	305	3.67	0.29	0.63	42.8	501.6	443	501.6	0	746
74	4572	1905	101.6	2.40	914	102	3.89	0.3	0.71	38.4	501.6	444	525	0	836
75	4572	1905	101.6	2.40	305	305	3.67	0.29	0.63	21.8	487.1	440	511.2	932.236	825
76	4572	1905	101.6	2.40	305	305	3.67	0.29	0.63	49.3	489.2	457	489.2	1195.456	980
77	4572	1905	101.6	2.40	305	305	3.67	0.29	1.38	42	453.4	447	481.6	1195.456	978
78	4572	1905	101.6	2.40	305	305	3.67	0.29	0.63	44.1	460.9	429	460.9	1195.456	977
79	4572	1905	152.4	2.40	305	305	3.67	0.2	0.42	51.8	460.9	429	460.9	1187.97	973
80	4572	1905	101.6	2.40	305	305	1.97	0.29	0.63	45.6	474.7	437	474.7	1195.456	707
81	4572	1905	101.6	2.40	914	102	4.35	0.31	0.63	45.6	463.7	429	463.7	1191.612	887
82	5486	1905	101.6	2.88	0	0	5.58	0.25	0.37	23.3	488.1	476	472.7	0	339
83	1750	700	100	2.50	0	0	0.45	0.72	0.44	27.4	445	445	608.9	287.4	144
84	1750	700	100	2.50	0	0	0.45	0.72	0.44	27.4	445	445	608.9	479	166
85	1750	700	100	2.50	0	0	0.45	0.72	0.44	27.4	445	445	608.9	671.6	186
86	1067	254	51	4.20	102	51	2.8	0.79	0.48	36.5	552	552	572.3	0	19
87	1067	254	51	4.20	102	51	2.8	0.79	0.48	36.5	552	552	572.3	0	17
88	1067	254	51	4.20	102	51	2.8	0.79	0.48	33.8	552	552	572.3	0	19
89	1067	254	51	4.20	102	51	2.8	0.79	0.48	32.4	552	552	572.3	0	16
90	1067	254	51	4.20	102	51	2.8	0.79	0.48	31.7	552	552	572.3	0	19
91	1067	254	51	4.20	102	51	2.8	0.79	0.48	30.3	552	552	572.3	0	15
92	2525	1020	120	2.48	300	300	2.68	0.22	0.62	38.3	411	389	411	540	440
93	6096	2286	152.4	2.67	0	0	4.41	0.39	0.49	54.3	441	441	411	0	838
94	6096	2286	152.4	2.67	0	0	4.41	0.39	0.49	57.5	441	441	411	0	890
95	6096	2286	152.4	2.67	0	0	4.41	0.39	0.49	56	441	441	411	0	815
96	4572	1905	101.6	2.40	0	0	6	0.22	0.42	24.4	483	517	517	329.168	568
97	4572	1905	101.6	2.40	0	0	3.5	0.28	0.31	22.7	483	490	517	329.168	282
98	4572	1905	101.6	2.40	305	305	3.67	0.29	0.63	53.8	517	436	517	48.93	726
99	4572	1905	101.6	2.40	305	305	3.67	0.29	0.63	41.7	517	432	517	48.93	792
100	4572	1905	101.6	2.40	914	102	2.29	0.25	0.31	27.9	483	517	517	596.062	421
101	2540	1016	76	2.50	254	254	5.55	1.47	1.84	45.9	458	447	458.4	578.269	812
102	2540	1016	76	2.50	254	254	5.55	1.47	1.84	38.9	458	447	458.4	578.269	854
103	2540	1016	76	2.50	254	254	5.55	1.47	1.84	56.4	544.3	448	544.7	578.269	747
104	2540	1016	76	2.50	254	254	5.55	1.47	1.84	101.6	544.3	448	544.7	578.269	936
105	2540	1016	76	2.50	254	254	5.3	1.47	1.84	80.1	503	439	503.3	578.269	818
106	2540	1016	76	2.50	254	254	5.55	1.47	1.84	101.3	509.9	420	510.2	578.269	993
107	2540	1016	76	2.50	254	254	5.55	1.47	2.45	130.8	442.7	438	443	578.269	815
108	2540	1016	76	2.50	254	254	5.55	1.47	2.45	110.5	442.7	438	443	578.269	955
109	2700	1300	200	2.08	0	0	4.03	0.59	0.59	28.3	412	412	452	0	460

ID	H_w (mm)	L_w (mm)	t_w (mm)	H_w/L_w –	t_f (mm)	L_f (mm)	ρ_{vf} (%)	ρ_{vw} (%)	ρ_{hw} (%)	f_c' (MPa)	f_{yf} (MPa)	f_{yvw} (MPa)	f_{ywh} (MPa)	P (kN)	V (kN)
110	2700	1300	200	2.08	0	0	4.03	0.59	0.59	28.3	412	412	452	0	429
111	1140	548	84	2.08	0	0	3.56	0.71	0.67	47	412	450	450	0	83
112	1140	548	84	2.08	0	0	3.56	0.71	0.67	47	412	450	450	0	82
113	4560	2000	150	2.28	0	0	1.32	0.3	0.25	45	583.6	547	583.6	689	336
114	4560	2000	150	2.28	0	0	1.32	0.3	0.25	40.5	484.9	583	484.9	691	359
115	4560	2000	150	2.28	0	0	1.54	0.54	0.25	39.2	489	569	489	686	454
116	4560	2000	150	2.28	0	0	1.54	0.54	0.25	40.9	489	576	518.9	695	443
117	4560	2000	150	2.28	0	0	0.67	0.27	0.25	38.3	562.2	518	518.9	1474	439
118	4520	2000	150	2.26	0	0	1.54	0.54	0.25	45.6	518.9	576	518.9	1476	597
119	3315	1524	203.2	2.18	0	0	4.9	0.4	0.55	30.7	482.6	434	530.9	889.644	703
120	3315	1524	203.2	2.18	0	0	4.9	0.4	0.55	30.3	482.6	434	530.9	889.644	694
121	3315	1524	203.2	2.18	0	0	4.9	0.4	0.55	33.8	482.6	434	530.9	889.644	707
122	3315	1524	203.2	2.18	0	0	4.9	0.4	0.55	31.4	482.6	462	530.9	889.644	721
123	3315	1524	203.2	2.18	0	0	4.9	0.4	0.55	31	482.6	462	530.9	889.644	721
124	3315	1524	203.2	2.18	0	0	4.9	0.4	0.55	31.7	482.6	462	455.1	889.644	756
125	1500	700	100	2.14	0	0	0.88	0.67	1.01	36.8	405	405	305	498.96	201
126	1500	700	100	2.14	0	0	0.65	0.67	1.01	40.2	405	405	305	784	224
127	1500	700	100	2.14	0	0	1.8	0.67	1.01	43.1	405	405	305	594.72	304
128	1500	700	100	2.14	0	0	1.53	0.67	1.01	34.7	405	405	305	688.45	266
129	1750	700	75	2.50	0	0	0.49	0.67	0.46	27.4	445	445	523.9	216	113
130	1750	700	100	2.50	0	0	0	1.34	0.44	27.4	445	445	608.9	287	138
131	1750	700	100	2.50	0	0	0.45	0.72	0.44	27.4	445	445	608.9	287	149
132	1750	700	100	2.50	0	0	0.45	0.72	0.64	27.4	608.9	445	608.9	287	156
133	1750	700	100	2.50	0	0	0.45	0.72	0.56	27.4	445	445	608.9	287	145
134	4500	1500	200	3.00	0	0	1.27	0.32	0.28	36.9	335	335	335	1107	321
135	2900	1000	75	2.90	0	0	2.33	0.91	0.91	24.1	289	289	289	200	125
136	2900	1000	75	2.90	0	0	2.33	0.91	0.91	24.9	289	289	289	200	90
137	3000	1000	60	3.00	0	0	9.4	0.4	0.4	12.3	452.9	365	452.9	220	92
138	3000	1000	60	3.00	120	120	4.7	0.4	0.4	12.8	450.8	365	452.9	180	117
139	3000	1000	60	3.00	420	60	2.39	0.4	0.4	12.8	452.9	365	452.9	115	137
140	2350	900	75	2.61	0	0	3.72	0.7	0.84	37.3	526	526	345	400	140
141	2350	900	75	2.61	0	0	3.72	0.7	0.84	37.3	526	526	345	0	155
142	2350	900	75	2.61	0	0	3.72	0.7	0.42	37.3	526	526	345	0	137
143	2350	900	75	2.61	0	0	3.72	0.7	0.42	37.3	526	526	345	400	169
144	1650	700	125	2.36	325	125	4.83	1.21	1.26	32	285	341	285	400	345
145	1650	700	125	2.36	325	125	4.83	1.21	1.8	32	285	341	285	400	379
146	1100	500	50	2.20	0	0	2.24	0.28	0.28	21.6	276	276	216	0	15
147	1100	500	50	2.20	0	0	2.24	0.28	0.28	21.6	276	276	216	0	20
148	1100	500	50	2.20	0	0	2.24	0.28	0.28	22.5	276	276	216	0	18
149	1100	500	50	2.20	0	0	2.24	0.28	0.28	23.5	276	276	216	0	20
150	6401	1905	76	3.36	0	0	0.27	0.27	0.27	51.2	415.1	415.1	422.6	415.353	118
151	6401	1905	76	3.36	0	0	1	1	0.27	47.4	450.9	450.9	420.6	430.365	184
152	6401	1905	76	3.36	0	0	3	3	0.27	46.7	455.1	455.1	413.7	420.357	294
153	6401	1905	76	3.36	0	0	7.67	1	0.27	41	434.4	434.4	482.6	430.365	322
154	4384	1572	57	2.79	143	143	1.11	0.33	0.47	31.7	448	448	510	178	106

Author contributions SMN: conceptualization, methodology, visualization, writing—original draft. N-LT: methodology, software, validation, writing—original draft. T-HN: conceptualization, software, writing—original draft. V-BT: validation, visualization. D-DN: methodology, formal analysis, writing—review and editing, supervision.

Funding No funding was used in this study.

Data availability Data will be made available on request.

Declarations

Conflict of interest The authors declare that they have no conflicts of interest.

References

- ACI-318 (2014). ACI 318–14: Building Code Requirements for Structural Concrete and Commentary. American Concrete Institution Indianapolis, IN, USA.
- Adorno-Bonilla, C.M. (2016). Shear strength and displacement capacity of squat reinforced concrete shear walls. (UNIVERSITY OF PUERTO RICO MAYAGÜEZ CAMPUS).
- ASCE, SEI-43-05. (2005). *Seismic design criteria for structures, Systems, and Components in Nuclear Facilities*. American Society of Civil Engineers.
- Breiman, L. (2001). Random forests. *Machine Learning*, 45, 5–32.
- Burden, F., and Winkler, D. (2009). Bayesian regularization of neural networks. *Artificial neural networks: methods and applications*, 23–42.
- Chatterjee, S., Sarkar, S., Hore, S., Dey, N., Ashour, A. S., & Balas, V. E. (2017). Particle swarm optimization trained neural network for structural failure prediction of multistoried RC buildings. *Neural Computing and Applications*, 28, 2005–2016.
- Chen, T., and Guestrin, C. (2016). Xgboost: A scalable tree boosting system. pp. 785–794.
- Chen, X., Fu, J., Yao, J., & Gan, J. (2018). Prediction of shear strength for squat RC walls using a hybrid ANN–PSO model. *Engineering with Computers*, 34, 367–383.
- Chou, J.-S., Liu, C.-Y., Prayogo, H., Khasani, R. R., Gho, D., & Lalitan, G. G. (2022). Predicting nominal shear capacity of reinforced concrete wall in building by metaheuristics-optimized machine learning. *Journal of Building Engineering*, 61, 105046.
- EN-1998-1 (2004). Eurocode 8: Design of Structures for Earthquake Resistance - Part 1: General Rules. Seismic Actions and Rules for Buildings.
- Falcone, R., Lima, C., & Martinelli, E. (2020). Soft computing techniques in structural and earthquake engineering: A literature review. *Engineering Structures*, 207, 110269.
- Farzinpour, A., Dehcheshmeh, E. M., Broujerdian, V., Esfahani, S. N., & Gandomi, A. H. (2023). Efficient boosting-based algorithms for shear strength prediction of squat RC walls. *Case Studies in Construction Materials*, 18, e01928.
- Gulec, C.K., and Whittaker, A.S. (2011). Empirical equations for peak shear strength of low aspect ratio reinforced concrete walls. *ACI Structural Journal*, 108.
- Gulec, C. K., Whittaker, A. S., & Stojadinovic, B. (2008). Shear strength of squat rectangular reinforced concrete walls. *ACI Structural Journal*, 105, 488.
- Kassem, W. (2015). Shear strength of squat walls: A strut-and-tie model and closed-form design formula. *Engineering Structures*, 84, 430–438.
- Kaveh, A., and Khavaninzadeh, N. (2023). Efficient training of two ANNs using four meta-heuristic algorithms for predicting the FRP strength. (Elsevier), pp. 256–272.
- Kaveh, A., Eskandari, A., and Movasat, M. (2023). Buckling resistance prediction of high-strength steel columns using metaheuristic-trained artificial neural networks. (Elsevier), pp. 104853.
- Kaveh, A., DadrasEslamlou, A., Javadi, S., & Geran Malek, N. (2021). Machine learning regression approaches for predicting the ultimate buckling load of variable-stiffness composite cylinders. *Acta Mechanica*, 232, 921–931.
- Keshtegar, B., Nehdi, M. L., Trung, N.-T., & Kolahchi, R. (2021). Predicting load capacity of shear walls using SVR–RSM model. *Applied Soft Computing*, 112, 107739.
- Mangalathu, S., Jang, H., Hwang, S.-H., & Jeon, J.-S. (2020). Data-driven machine-learning-based seismic failure mode identification of reinforced concrete shear walls. *Engineering Structures*, 208, 110331.
- Moradi, M. J., & Hariri-Ardebili, M. A. (2019). Developing a library of shear walls database and the neural network based predictive meta-model. *Applied Sciences*, 9, 2562.
- Nguyen, D.-D., Tran, V.-L., Ha, D.-H., Nguyen, V.-Q., & Lee, T.-H. (2021). A machine learning-based formulation for predicting shear capacity of squat flanged RC walls. *Structures*, 29, 1734–1747.
- Nguyen, T.-H., & Nguyen, D.-D. (2023). Improved data-driven models for estimating shear capacity of squat rectangular reinforced concrete walls. *Asian Journal of Civil Engineering*. <https://doi.org/10.1007/s42107-023-00941-6>
- Ranganathan, A. (2004). The levenberg-marquardt algorithm. *Tutorial on LM Algorithm*, 11, 101–110.
- Sánchez-Alejandre, A., & Alcocer, S. M. (2010). Shear strength of squat reinforced concrete walls subjected to earthquake loading—trends and models. *Engineering Structures*, 32, 2466–2476.
- Tariq, M., Khan, A., Ullah, A., Zamin, B., Kashyadeh, K. R., & Ahmad, M. (2022). Gene Expression Programming for Estimating Shear Strength of RC Squat Wall. *Buildings*, 12, 918.
- Thai, H.-T. (2022). Machine learning for structural engineering: A state-of-the-art review. (Elsevier), pp. 448–491.
- Wood, S. L. (1990). Shear strength of low-rise reinforced concrete walls. *Structural Journal*, 87, 99–107.

Publisher's Note Springer Nature remains neutral with regard to jurisdictional claims in published maps and institutional affiliations.

Springer Nature or its licensor (e.g. a society or other partner) holds exclusive rights to this article under a publishing agreement with the author(s) or other rightsholder(s); author self-archiving of the accepted manuscript version of this article is solely governed by the terms of such publishing agreement and applicable law.